

Article

A Comparison of Hořava–Lifshitz Gravity and Einstein Gravity through the Gravitational Deflection of Massive Body around Black Holes

Safiqul Islam ^{1,*} and Farook Rahaman ² 

¹ Department of Basic Sciences, Deanship of Preparatory Year, King Faisal University, Hofuf 31982, Al-Hasa, Saudi Arabia

² Department of Mathematics, Jadavpur University, Kolkata 700032, West Bengal, India; rahaman@associates.iucaa.in

* Correspondence: sislam@kfu.edu.sa

Abstract: Hořava has proposed a renormalizable gravity theory with higher spatial derivatives in four dimensions. This theory may be regarded as a UV complete candidate for general relativity. After the proposal of this theory, Kehagias and Sfetsos have found a new asymptotically flat black hole solution in Hořava–Lifshitz gravity. In recent times, a new test of gravity theory is suggested that assumes the deflection of the massive body around a black hole. In this paper, we will study the effect of the Hořava–Lifshitz parameters on the black hole deflection angle and emphasize those features that permit a comparison of Hořava–Lifshitz to Einstein gravity.

Keywords: Hořava–Lifshitz theory; black hole; Jacobi metric; deflection of massive particle

MSC: 83A05; 83-10; 83C56; 83C57; 83F05



Citation: Islam, S.; Rahaman, F. A Comparison of Hořava–Lifshitz Gravity and Einstein Gravity through the Gravitational Deflection of Massive Body around Black Holes. *Axioms* **2023**, *12*, 364. <https://doi.org/10.3390/axioms12040364>

Academic Editors: Angel Ricardo Plastino and Palle E. T. Jorgensen

Received: 7 March 2023

Revised: 1 April 2023

Accepted: 7 April 2023

Published: 10 April 2023



Copyright: © 2023 by the authors. Licensee MDPI, Basel, Switzerland. This article is an open access article distributed under the terms and conditions of the Creative Commons Attribution (CC BY) license (<https://creativecommons.org/licenses/by/4.0/>).

1. Introduction

Recently, Hořava [1] has proposed a renormalizable gravity theory with higher spatial derivatives in four dimensions. This theory may be regarded as a UV complete candidate for general relativity. It has received utmost attention, and since it was formulated, various properties and characteristics have been put forth. Jafarzade et al. [2] studied the Van der Waals fluid behavior in the Horava–Lifshitz (HL) black hole and hence modified the solution of the black hole with a cosmology ansatz. They considered the cosmological constant as the thermodynamical pressure and its conjugate quantity as the thermodynamical volume and observed that stability existed only in a special region of the black hole. The HL theory comes back to Einstein gravity with a non-vanishing cosmological constant in IR, but it has improved UV behaviors. In this theory, we ignore the local Lorentz symmetry incorporated in Einstein’s GTR and consider different kinds of temporal and spatial scaling at short distances. Quantum field theory has considerable experimental success, but it predicts infinite values for physical quantities from the theoretical point of view. This QFT of gravity with a dynamical critical exponent equal to $z = 3$ in the UV was further discussed in [3]. It was observed therein that the Newton constant, cosmological constant as well as the effective speed of light all arise from deformations of the nonrelativistic $z = 3$ theory at meager distances. Hořava [4] further extended the definition of spectral dimension to theories on smooth spacetimes by considering anisotropic scaling. It is observed that the spectral dimension of spacetime in quantum gravity, dominated by a Lifshitz point, is given by $d_s = 1 + \frac{D}{z}$ (where z is the dynamical critical exponent in $D + 1$ dimensions). The author [5] studied nonrelativistic Yang–Mills gauge theories in $(D + 1)$ dimensions, which in the large- N limit can have weakly curved gravity duals. The standard spherically symmetric Schwarzschild-(A)dS black hole solutions have also been observed in relation to the Hořava–Lifshitz theory.

Xu et al. [6] studied the evaporation process in HL gravity for various spacetime dimensions in a spherically symmetric neutral AdS black hole. Myung [7] investigated Lifshitz black holes under Hořava–Lifshitz gravity. By comparing a Lifshitz black hole with the 3D new massive gravity, the author found that all these black hole solutions have single horizons and are very much akin to each other as related to their thermodynamical property. Myung et al. [8] investigated black holes in Hořava–Lifshitz gravity considering a parameter λ . It was observed that for $1/3 \leq \lambda < 3$ they behave as Lifshitz black holes with a dynamical exponent $0 < z \leq 4$, while for $\lambda > 3$ they behave as an RN-type black hole where the spacetimes are asymptotically flat. Sadeghi et al. [9] investigated the entropy and Hawking temperature for two kinds of Hořava–Lifshitz black holes, Kehagias–Sfetsos (KS) and Lu–Mei–Pope. The Hawking temperature as well as the entropy was obtained in 4D spacetime by considering the effect of the back reaction on the surface gravity. Kiritsis et al. [10] found that the generic solution for Hořava–Lifshitz “Black Holes” has conventional (AdS, dS or flat) asymptotics with the universal $1/r$ tail.

Rindler et al. [11] studied the effect of the Λ (cosmological constant) on the bending of light around a spherically symmetric concentrated mass. It was found that when the Schwarzschild–de Sitter geometry is taken into consideration, Λ does contribute to the bending, even though this term gets canceled out in the photon geodesic equation. Rahaman et al. [12] constructed a new class of thin-shell wormholes from black holes in Hořava–Lifshitz gravity by employing the asymptotically flat Kehagias–Sfetsos (KS) solution for various values of the coupling constant ω and the mass M . It is observed that the radius of the outer event horizon in the KS case is less than that in the Schwarzschild case. Manna et al. [13] recently investigated the three classical tests of GR, the deflection of light, the precession of perihelion and time delay in Einstein–AEther gravity. Such Einstein–AEther gravity has two static and spherically symmetric charged black hole solutions which correspond to different constraints on the coupling constants. Sultana [14] examined the cosmological constant Λ and its effects on the deflection angle for null geodesics in the equatorial plane of Kerr–de Sitter spacetime when $\phi = 0$. It is seen that the cosmological constant contributes to the expression of the deflection angle.

According to the GTR, the gravitational field of a massive object causes light rays to bend, which passes by it. It influences the motion as well as the spectral properties of light by directly acting on a dynamic spacetime continuum through which light propagates. The deflection of light by mass was first calculated by German astronomer Johann Georg von Soldner in 1801 [15]. The author showed that rays from a distant star, while passing the Sun’s surface, would be deflected by an angle of around 0.9 arc seconds, or one-quarter of a thousandth degree. The gravitational deflection of light was predicted by Einstein in his general theory of relativity, in the early 20th century. Einstein calculated that the deflection predicted by his theory would be twice the Newtonian value. There are several methods such as null geodesics (under both strong field and weak field approximations) and material medium methods to calculate the deflection of a light ray as it passes around a gravitational mass. Jusufi et al. [16] investigated weak gravitational lensing for a wormhole and a black hole in the presence of massive gravity. It is found that the black hole solution is dependent on the parameter λ , scalar charge S and mass M . Further, it is observed that as S vanishes, the Schwarzschild geometry is recovered. Conformal Weyl gravity is considered as a possible alternative to the standard second-order Einstein GTR. The bending angle of light associated with the metric of a centrally concentrated spherically symmetrical distribution of matter in a Schwarzschild–deSitter background was examined by Sultana et al. [17].

The gravitational deflection can be used to study various modified gravities. There are many other works related to this issue, such as in [18] where the authors observed that in the case of a Schwarzschild black hole, two infinite sets of relativistic images are formed, apart from the primary and secondary ones. Tsukamoto [19] reexamined the deflection angle in the Ellis wormhole spacetime and also obtained the value for the RN spacetime. A strong gravitational field deflection limit for photons in a Schwarzschild black hole was studied

by Lu et al. [20]. Strong deflection gravitational lensing nearby the event horizon of a BH provides some clues of the quantum effects in the central core. Zhao et al. [21] estimated the observables of the strong deflection lensing for the supermassive black hole in the Galactic Center. Gravitational lensing in the KS spacetime using the framework of Hořava–Lifshitz gravity was investigated by Horváth [22]. Weak and strong deflection limits for the deflection angle were found by Eiroa et al. [23]. The positions and magnifications of the images were calculated and the results were compared with those corresponding to the Schwarzschild and RN spacetimes. Zhao et al. [24] observed that the Lee–Wick BH can be distinguished from the Schwarzschild BH through the effects of lensing when the UV scale is not very large. Strong deflection gravitational lensing was further studied by Zhu et al. [25] in the presence of a Lee–Wick ultracompact object. They obtained its observables and estimated them for the supermassive BHs Sgr A* and M87*. Strong deflection gravitational lensing through an Einstein–Lovelock ultracompact object was investigated by Gao et al. [26]. They found that the relativistic images inside the photon sphere are absent for an Einstein–Lovelock BH. Zhao et al. [27] observed the gravitational lensing caused by a charged Galileon BH and hence calculated the time delays and angular separations between the relativistic images of the charged Galileon BH.

In the field of weak deflection gravitational lensing, there is another method to calculate the deflection angle and observables, such as Keeton and Petters’ formalism [28–30]. The strong and weak deflection gravitational lensings of the regular black hole were investigated by Liu et al. [31]. The authors found that its weak deflection lensing is the same as that of a Reissner–Nordström black hole. Lu et al. [32] considered the supermassive black holes Sgr A* and M87* in the Galactic Center and at the center of M87 as lenses and hence observed the weak and strong deflection gravitational lensing. The authors also observed in [33] that the time delay in weak deflection lensing depends strongly on the phantom hair, but the delay in the strong deflection lensing depends on the hair and strength of the coupling. Gao et al. [34] investigated the strong and weak deflection gravitational lensing in the Einstein–scalar–Gauss–Bonnet gravity by the hairy black holes, using five types of coupling functions. Lu et al. [35] further investigated strong and weak deflection gravitational lensing by the quantum deformed Schwarzschild BH. Considering Sgr A* as the lens, they measured the angular difference, angular separation, time delay and the fluxes difference. Wang et al. [36] considered a supermassive BH in the Galactic Center as the lens and evaluated the weak and strong deflection lensing observables. These signatures are compared with those of the Schwarzschild, RN, tidal RN and charged Galileon BHs. A test of $f(T)$ gravity by studying the gravitational time advancement was performed by Deng [37]. The author used dual-way light propagation between an observer and a distant spacecraft and hence measured the light traveling time as the observer’s proper time. Zhang et al. [38] investigated strong and weak deflection gravitational lensing by a black-bounce–RN spacetime and obtained their lensing observables. Further studies on deflection gravitational lensing were conducted by various authors in [39,40].

Harko et al. [41] investigated the possibility of observational constraints on Hořava gravity. Classical tests of GR are considered for the spherically symmetric black hole Kehagias–Sfetsos solution of HL gravity. Such gravitational effects can be studied in the framework of the vacuum solution of HL gravity. The HL theory is invariant in time and space and hence exhibits a broken Lorentz symmetry at a short distance. Moreover, at large distances, the higher derivative terms have no contribution, and the theory reduces to the standard GR theory. In this present study, we would like to investigate the total deflection angle when the HL parameters are $\phi \rightarrow \infty$ or $\omega \rightarrow \infty$; the latter however is the Schwarzschild case. The impact of the relativistic gravitational deflection of light was studied by Turyshev [42], on the accuracy of the future Space Interferometry Mission (SIM). The deflection angles caused by the monopole, quadrupole and octupole components of gravitational fields, for a number of massive celestial bodies in the solar system, are measured.

We organize our paper as follows. In Section 2, we briefly discuss the HL black holes. The deflection of the massive body is studied in detail in Section 3. The concluding remarks are in Section 4. Throughout the paper, the geometrized units $G = c = 1$ are considered.

2. Hořava–Lifshitz Black Holes

Hořava–Lifshitz gravity (also known as Hořava gravity) is a quantum gravity theory proposed by Peter Hořava in 2009 [3]. The problem that arises out of different concepts of time in quantum field theory and GR is solved, where the quantum concept is considered more fundamental. This relativistic concept of time emerges at large distances with its Lorentz invariance. Hence, space and time are anisotropic at a high energy level. Hořava–Lifshitz gravity indeed explains the current acceleration and major cosmic issues and is hence considered a very interesting proposal of modified gravity theory. In terms of the AdS/CFT correspondence [43], Hořava–Lifshitz black holes are very useful to model holographic superconductors considering the symmetry of Lifshitz scaling. It is useful to study the stability of HL black holes in the context of AdS/CFT. Uncharged topological black holes in HL theory are stable, as compared to their counterparts in Einstein gravity. Black hole thermodynamics in HR gravity has been discussed by Cai et al. [44]. The mass, entropy of the black holes and λ , the dynamical coupling constant, are obtained in HR gravity. It is observed that such black holes are thermodynamically stable in some parameter space, whereas in some other parameter space they are unstable. The relation between the horizon area of the black holes and entropy is also deduced.

The Hořava–Lifshitz action [45] defines a nonrelativistic and renormalizable gravitation theory given by

$$S = \int \sqrt{-g}N \left[\frac{2}{\sigma^2} (K_{ij}K^{ij} - \lambda_g K^2) + \epsilon^{ijk} \frac{\sigma^2 \mu}{2\nu_g^2} R_{il} \nabla_j R^l_\sigma - \frac{\sigma^2 \mu^2}{8} R_{ij}R^{ij} + \left(\frac{4\lambda_g - 1}{4} R^2 - \Lambda_W R + 3\Lambda_W^2 \right) \frac{\sigma^2 \mu^2}{8(3\lambda_g - 1)} - \frac{\sigma^2}{2\nu_g^4} C_{ij}C^{ij} \right] dt dx^3 \tag{1}$$

where N is the lapse function; $\sigma, \lambda_g, \nu_g, \mu, \Lambda_W$ are the constant parameters; the Cotton tensor denoted by $C_{ij} = \epsilon^{ikl} \nabla_k (R^j_l - \frac{1}{4} R \delta^j_l)$; R_{ijkl} is the 3D curvature tensor; and the extrinsic curvature is defined by $K_{ij} = \frac{1}{2N} (\dot{g}_{ij} \nabla_i N_j - \nabla_j N_i)$, the dot being the derivative with respect to t .

We consider a static and spherically symmetric solution given by

$$ds^2 = -e^{\nu(r)} dt^2 + e^{\lambda(r)} dr^2 + r^2 (d\theta^2 + \sin^2 \theta d\phi^2), \tag{2}$$

where the functions $\nu(r)$ and $\lambda(r)$ are the metric potentials.

Now, by imposing $\lambda_g = 1$, which reduces to the Einstein–Hilbert action in the infrared limit, one obtains the following solution of the vacuum field equations in Hořava gravity [46]:

$$e^{\nu(r)} = e^{-\lambda(r)} = 1 + (\omega - \Lambda_W)r^2 - \sqrt{r[\omega(\omega - 2\Lambda_W)r^3 + \beta]} \tag{3}$$

Here, β is an integration constant and Λ_W and ω are constant parameters. Now, the Kehagias–Safetsos (KS) black hole solution [47] is obtained by considering $\beta = 4\omega M$ and $\Lambda_W = 0$ as

$$e^{\nu(r)} = 1 + \omega r^2 - \omega r^2 \sqrt{1 + \frac{4M}{\omega r^3}} \tag{4}$$

By considering $\beta = -\frac{\omega^2}{\Lambda_W}$ and $\omega = 0$, the solution given by Equation (3) reduces to the Lu, Mei and Pope (LMP) solution [48], given by

$$e^{v(r)} = 1 - \Lambda_W r^2 - \frac{\alpha^2}{\sqrt{-\Lambda_W}} \sqrt{r} \tag{5}$$

The Kehagias–Sfetsos solution is the only asymptotically flat solution in the family of solutions (2). We shall use the Kehagias–Sfetsos solution for analyzing the behavior of massive and massless test particles around Hořava–Lifshitz black holes. It is to be noted that there is an outer (event) horizon and an inner (Cauchy) horizon of Kehagias–Sfetsos black hole solutions at r where $f(r) \equiv e^{v(r)} = 1 + \omega r^2 - \omega r^2 \sqrt{1 + \frac{4M}{\omega r^3}} = 0$,

$$r_{\pm} = M \left[1 \pm \sqrt{1 - \frac{1}{2\omega M^2}} \right]. \tag{6}$$

Equation (4) implies that if one takes $\frac{4M}{\omega r^3} \ll 1$, then

$$e^{v(r)} = 1 - \frac{2M}{r} \tag{7}$$

In other words, either large distance or $\omega M^2 \gg 1$, Hořava–Lifshitz black holes approach Schwarzschild black hole.

3. Outline of the Study of Deflection of Massive Body

For the study of deflection of massive body, at first one requires constructing Jacobi metric, which can be achieved from standard spacetime metric.

To find the Jacobi metric from the fundamental tensor

$$ds^2 = c^2 V^2(x) dt^2 - g_{ij}(x) dx^i dx^j, \tag{8}$$

we can write the Lagrangian for a massive particle corresponding to this metric as

$$L(x, \dot{x}) = m \sqrt{c^2 V^2(x) \dot{t}^2 - g_{ij} \dot{x}^i \dot{x}^j}. \tag{9}$$

(Here, V is the potential energy). The action for a massive particle

$$S = -m \int L dt, \tag{10}$$

yields the canonical momentum conjugate as

$$\frac{H}{c} = \frac{E}{c} = \frac{\partial L}{\partial \dot{t}} = \frac{m c^2 V^2(x) \dot{t}}{\sqrt{c^2 V^2(x) \dot{t}^2 - g_{ij} \dot{x}^i \dot{x}^j}}; \quad \frac{p_i}{c} = \frac{\partial L}{\partial \dot{x}^i} = \frac{-m g_{ij} \dot{x}^j}{\sqrt{c^2 V^2(x) \dot{t}^2 - g_{ij} \dot{x}^i \dot{x}^j}} \tag{11}$$

The above equations yield the relativistic energy equation in curved spacetime

$$\frac{E^2}{c^2} - m^2 c^2 V^2(x) = V^2(x) g^{ij}(x) p_i p_j \quad \text{or,} \quad \frac{c^2 V^2 g^{ij}(x)}{E^2 - m^2 c^4 V^2(x)} p_i p_j = 1 \tag{12}$$

With $p_i = \partial_i S$, this provides the Hamilton Jacobi equation for the geodesics as

$$\frac{V^2 g^{ij} \partial_i S \partial_j S}{E^2 - m^2 V^2} = 1, \tag{13}$$

with Jacobi metric J_{ij} given by

$$J^{ij}(x) = \frac{V^2(x) g^{ij}(x)}{E^2 - m^2 V^2(x)}. \tag{14}$$

For massless particle, i.e., when $m = 0$, the Jacobi metric assumes the form

$$J_{ij} = \frac{E^2}{V^2} g_{ij}. \tag{15}$$

This is known as optical or fermat metric [49]. In Jacobi metric approach, energy plays a role of supplementary parameter as Jacobi metric comprises kinetic energy explicitly.

For a general static spherically symmetric metric

$$ds^2 = -A(r)dt^2 + B(r)dr^2 + C(r)(d\theta^2 + \sin^2\theta d\phi^2), \tag{16}$$

the Jacobi metric assumes the form

$$J_{ij}dx^i dx^j = (E^2 - m^2 A) \left[\frac{B}{A} dr^2 + \frac{C}{A} (d\theta^2 + \sin^2\theta d\phi^2) \right]. \tag{17}$$

(Here, $A = e^{\nu(r)}$, $B = e^{\lambda(r)}$, $C = r^2$ defined in Equation (3)). As usual, we study the motion of the massive particle in the equatorial plane $\theta = \pi/2$. As a result, Jacobi metric takes the form as

$$ds^2 = (E^2 - m^2 A) \left(\frac{B}{A} dr^2 + \frac{C}{A} d\phi^2 \right). \tag{18}$$

Due to axial symmetry, the angular momentum (J) for the motion is conserved which is given as

$$J = (E^2 - m^2 A) \frac{C}{A} \frac{d\phi}{ds} = \text{constant}. \tag{19}$$

Moreover, from Jacobi metric (17), we find

$$(E^2 - m^2 A)^2 \frac{B}{A} \left(\frac{dr}{ds} \right)^2 = E^2 - A \left(m^2 + \frac{J^2}{C} \right). \tag{20}$$

Now, finally, we obtain the trajectory (by using $U = \frac{1}{r}$) as,

$$\left(\frac{dU}{d\phi} \right)^2 = \frac{C^2 U^4}{AB} \left[\left(\frac{\alpha}{\beta} \right)^2 - A \left(\frac{1}{\beta^2} + \frac{1}{C} \right) \right]. \tag{21}$$

Here, the quantities $\beta = \frac{J}{m}$ and $\alpha = \frac{E}{m}$ represent the angular momentum and angular energy per unit mass, respectively.

Let a massive particle having mass m come from an asymptotically flat region. Following geodesic path, the particle with velocity v reaches near the black hole at a minimal distance b and continues the journey up to the viewer at far distance, and then its energy is

$$E = \frac{m}{\sqrt{1 - v^2}} \quad [\text{assuming } c = 1]. \tag{22}$$

In a similar manner, the particle's angular momentum is

$$J = \frac{m v b}{\sqrt{1 - v^2}}. \tag{23}$$

Hence, the Jacobi metric assumes the form as

$$ds^2 = m^2 \left(\frac{1}{1 - v^2} - A \right) \left[\frac{B}{A} dr^2 + \frac{C}{A} d\phi^2 \right]. \tag{24}$$

Hence, the trajectory of the massive particle can be written as

$$\left(\frac{dU}{d\phi}\right)^2 = \frac{C^2 U^4}{AB} \left[\frac{1}{v^2 b^2} - A \left(\frac{1-v^2}{v^2 b^2} + \frac{1}{C} \right) \right] \equiv f(U). \tag{25}$$

For $v \rightarrow 1$, this equation transforms to null geodesic equation.

The conditions for circular orbit are

$$f(U) = 0 \text{ and } f'(U) = 0. \tag{26}$$

at some $U = U_c$.

One can rewrite this equation as

$$\frac{d^2 U}{d\phi^2} + U = F(U), \text{ where } F(U) = U + \frac{1}{2} \frac{df}{dU}. \tag{27}$$

Now, employing our black hole solution, we try to solve this equation by using standard perturbation theory.

Following the Rindler–Ishak method [11], one can calculate the deflection angle of massive particles. Such gravitational deflection of a massive particle in Schwarzschild–de Sitter spacetime has been observed via the Rindler–Ishak method in the presence of a weak field [50]. Figure 1 indicates that the angle between radial direction (x^i) and direction of the particle motion (y^i) is ψ , where

$$\cos \psi = \frac{g_{ij} x^i y^j}{\sqrt{g_{ij} x^i x^j} \sqrt{g_{ij} y^i y^j}}. \tag{28}$$

Here, g_{ij} is the Hořava–Lifshitz black hole spacetime. Here, we assume $t = \text{constant}$, $\theta = \pi/2$ surface.

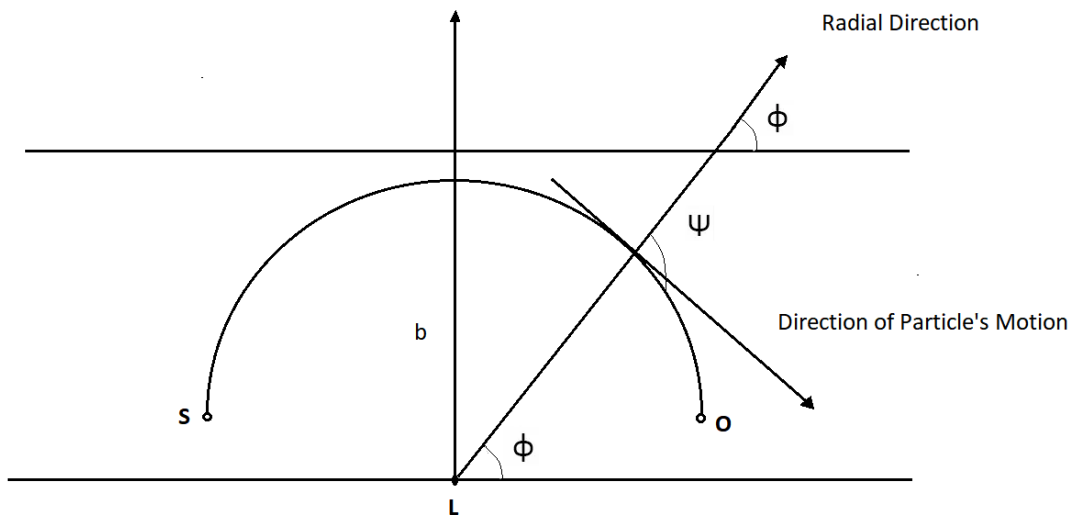


Figure 1. Schematic diagram of the orbital motion of the massive particle (here in the weak field limit, i.e., closest approach \approx impact parameter, b).

Note that

$$x^i = (dr, d\phi) = (\gamma, 1)d\phi, \text{ and } y^i = (dr, 0) = (1, 0)dr,$$

where $\gamma = \frac{dr}{d\phi}$.

Now, Equation (27) assumes the form

$$\cos \psi = \frac{|\gamma|}{\sqrt{\gamma^2 + \frac{g_{\phi\phi}}{g_{rr}}}} \text{ or } \tan \psi = \frac{\sqrt{\frac{g_{\phi\phi}}{g_{rr}}}}{|\gamma|}. \tag{29}$$

According to Figure 1, one can note that one side of gravitational deflection angle is

$$\epsilon = \psi(\phi) - \phi \tag{30}$$

Hence, 2ϵ is the total deflection angle.

4. Deflection of Massive Body around Hořava–Lifshitz Black Holes

Now, we try to calculate the deflection of massive body around Hořava–Lifshitz black holes. Using Kehagias–Safetsos (KS) black hole solution (4) in Equation (27), we obtain the trajectory of the massive particle as

$$\frac{d^2U}{d\phi^2} + U = -\left(\frac{\omega}{U} - \frac{\omega}{U}\sqrt{1 + \frac{4MU^3}{\omega}}\right) + \left(\frac{\omega}{U^3} + \frac{3M}{\sqrt{1 + \frac{4MU^3}{\omega}}} - \frac{\omega}{U^3}\sqrt{1 + \frac{4MU^3}{\omega}}\right)\left(\frac{1 - v^2}{v^2b^2} + U^2\right). \tag{31}$$

First, as a zeroth approximation, when the terms on the right-hand side of the above differential equation are neglected, the solution is given as

$$U = \frac{\sin\phi}{b} \tag{32}$$

where b is the impact parameter. This is the solution when the path of the particle is a straight line path devoid of deflection, in the absence of the gravitating black hole. For the next approximation, we replace U on the right-hand side of Equation (30) with the zeroth solution in Equation (31); hence, we derive the following equation.

$$\begin{aligned} \frac{d^2U}{d\phi^2} + U = & -\left(\frac{\omega b}{\sin\phi} - \frac{\omega b}{\sin\phi}\sqrt{1 + \frac{4M\sin^3\phi}{\omega b^3}}\right) \\ & + \left(\frac{\omega b^3}{\sin^3\phi} + \frac{3M}{\sqrt{1 + \frac{4M\sin^3\phi}{\omega b^3}}} - \frac{\omega b^3}{\sin^3\phi}\sqrt{1 + \frac{4M\sin^3\phi}{\omega b^3}}\right)\left(\frac{1 - v^2}{v^2b^2} + \frac{\sin^2\phi}{b^2}\right) \end{aligned} \tag{33}$$

Expanding the RHS of Equation (32) and neglecting higher-order terms ($O(\frac{M}{\omega b^3})$), we obtain

$$\begin{aligned} \frac{d^2U}{d\phi^2} + U = & \frac{3M}{2b^2} - \frac{3M}{2b^2}\cos 2\phi + \frac{M(1 - v^2)}{b^2v^2} - \frac{9M^2}{4\omega b^4} + \frac{3M^2}{\omega b^4}\cos 2\phi - \frac{3M^2}{4\omega b^4}\cos 4\phi \\ & - \frac{9M^2(1 - v^2)}{2\omega b^5v^2}\sin\phi + \frac{3M^2(1 - v^2)}{2\omega b^5v^2}\sin 3\phi. \end{aligned} \tag{34}$$

The solution of the differential Equation (33) is obtained as a combination of the particular solution and the approximation Equation (31), as

$$U(\phi) = \frac{\sin\phi}{b} + \frac{2M}{b^2} + \frac{M(1 - v^2)}{b^2v^2} - \frac{16M^2}{5\omega b^4} - \frac{75M^2(1 - v^2)}{16\omega b^5v^2} + \frac{9M^2(1 - v^2)\phi\cos\phi}{2\omega b^5v^2}. \tag{35}$$

Hence, we finally obtain

$$\begin{aligned} \psi(\phi) = & \tan^{-1} \left[\left(\frac{2M}{b} + \frac{M(1-v^2)}{bv^2} - \frac{16M^2}{5\omega b^3} - \frac{75M^2(1-v^2)}{16\omega b^4 v^2} + \frac{9M^2(1-v^2)\phi \cos\phi}{2\omega b^4 v^2} + \sin\phi \right) \right. \\ & \times \left(1 - \left(\frac{M}{b^2 v^2} + \frac{M(1-v^2)}{2b^2 v^4} - \frac{8M^2}{5\omega b^4 v^2} - \frac{75M^2(1-v^2)}{32\omega b^5 v^4} + \frac{9M^2(1-v^2)\phi \cos\phi}{4\omega b^5 v^4} + \frac{\sin\phi}{2bv^2} \right) \right. \\ & \left. \left. \times \left(\frac{16M^2 v^2}{5\omega b^2} + \frac{75M^2(1-v^2)}{16\omega b^3} - \frac{9M^2(1-v^2)\phi \cos\phi}{2\omega b^3} - Mv^2 - bv^2 \sin\phi \right) \right) \right]. \end{aligned} \tag{36}$$

When $\phi = 0$,

$$U(\phi = 0) = \frac{2M}{b^2} + \frac{M(1-v^2)}{b^2 v^2} - \frac{16M^2}{5\omega b^4} - \frac{75M^2(1-v^2)}{16\omega b^5 v^2}. \tag{37}$$

Thus, at $\phi = 0$,

$$\begin{aligned} \psi(0) = & \tan^{-1} \left[\left(\frac{2M}{b} + \frac{M(1-v^2)}{bv^2} - \frac{16M^2}{5\omega b^3} - \frac{75M^2(1-v^2)}{16\omega b^4 v^2} \right) \right. \\ & \left. \times \left(1 - \left(\frac{M}{b^2 v^2} + \frac{M(1-v^2)}{2b^2 v^4} - \frac{8M^2}{5\omega b^4 v^2} - \frac{75M^2(1-v^2)}{32\omega b^5 v^4} \right) \left(\frac{16M^2 v^2}{5\omega b^2} + \frac{75M^2(1-v^2)}{16\omega b^3} - Mv^2 \right) \right) \right]. \end{aligned} \tag{38}$$

From Equation (35) and above, we find

$$\begin{aligned} \epsilon = & \tan^{-1} \left[\left(\frac{2M}{b} + \frac{M(1-v^2)}{bv^2} - \frac{16M^2}{5\omega b^3} - \frac{75M^2(1-v^2)}{16\omega b^4 v^2} + \frac{9M^2(1-v^2)\phi \cos\phi}{2\omega b^4 v^2} + \sin\phi \right) \right. \\ & \times \left(1 - \left(\frac{M}{b^2 v^2} + \frac{M(1-v^2)}{2b^2 v^4} - \frac{8M^2}{5\omega b^4 v^2} - \frac{75M^2(1-v^2)}{32\omega b^5 v^4} + \frac{9M^2(1-v^2)\phi \cos\phi}{4\omega b^5 v^4} + \frac{\sin\phi}{2bv^2} \right) \right. \\ & \left. \left. \times \left(\frac{16M^2 v^2}{5\omega b^2} + \frac{75M^2(1-v^2)}{16\omega b^3} - \frac{9M^2(1-v^2)\phi \cos\phi}{2\omega b^3} - Mv^2 - bv^2 \sin\phi \right) \right) \right] - \phi. \end{aligned} \tag{39}$$

Equation (39) gives the analytical expression of the gravitational deflection angle of the relativistic massive particle.

When $\phi = 0$, $\epsilon = \psi(0)$, i.e., then

$$\begin{aligned} \epsilon = & \tan^{-1} \left[\left(\frac{2M}{b} + \frac{M(1-v^2)}{bv^2} - \frac{16M^2}{5\omega b^3} - \frac{75M^2(1-v^2)}{16\omega b^4 v^2} \right) \right. \\ & \left. \times \left(1 - \left(\frac{M}{b^2 v^2} + \frac{M(1-v^2)}{2b^2 v^4} - \frac{8M^2}{5\omega b^4 v^2} - \frac{75M^2(1-v^2)}{32\omega b^5 v^4} \right) \left(\frac{16M^2 v^2}{5\omega b^2} + \frac{75M^2(1-v^2)}{16\omega b^3} - Mv^2 \right) \right) \right]. \end{aligned} \tag{40}$$

5. Conclusions and Discussions

We have found the expressions of the deflection angle of the asymptotically flat black hole solution in Hořava–Lifshitz gravity. We have started by showing the trajectory curves as a function of the impact parameter b , coupling constant ω , velocity of the particle v and black hole mass M . After that, we gave our attention to analyzing the impact of the aforementioned parameters on the deflection angle of the particle trajectory. Because our intention was to compare the deflection of a massive particle in Hořava–Lifshitz gravity with Einstein gravity, we compare our results graphically between the two gravity theories.

Note that as $\omega \rightarrow \infty$, the black hole solution in Hořava–Lifshitz gravity comes back to the Schwarzschild black hole solution, i.e., the black hole solution in Einstein gravity. Therefore, we try to explore graphically the Hořava–Lifshitz case and Einstein case. In Figure 2, we have shown the trajectory of the massive particle for different values of impact parameter b . The left panel shows the Hořava–Lifshitz case and the right panel shows the Einstein case. Figure 2 indicates that the flatness of the trajectory curve of the particle which is traveling under the gravitational field of the black hole in Hořava–Lifshitz gravity is more than the particle under the black hole in Einstein gravity. This implies that the gravitational field of the black hole in Hořava–Lifshitz gravity is less than the black hole in Einstein gravity. Figure 3 implies that the angle between the radial direction and the direction of particle motion is decreasing with the impact parameter in both Hořava–Lifshitz gravity and Einstein gravity. In Figure 4, one can note that the angle between the radial direction and the direction of the particle motion is decreasing with the mass of the black hole in Hořava–Lifshitz gravity, whereas it is increasing in Einstein gravity. From Figure 5, we see that the angle between the radial direction and the direction of particle motion is decreasing with the velocity of the test particle in both Hořava–Lifshitz gravity and Einstein gravity. Figures 6–8 reveal that the total deflection in Einstein gravity either for a general value of ϕ or a specific value of ϕ , say, $\phi = 0$, is more than Hořava–Lifshitz gravity. In Figure 9, we have shown a variation in the total deflection $2\epsilon(0)$ at $\phi = 0$ with respect to that of the coupling constant ω for different values of the impact parameter b . Note that the total deflection $2\epsilon(0)$ at $\phi = 0$ is increasing with respect to the coupling constant ω . The graphical representation of the variation in the total deflection angle throughout the spacetime as well as for a particular value at $\phi = 0$ are given in Figures 10–12. These figures exhibit the impact of the parameters on the deflection angle of the particle trajectory around the black hole in both gravity theories. Astronomical observations require a relativistic description of the propagation of light as well as the exact relativistic treatment of the massive celestial bodies and their dynamics.

The present study of the gravitational deflection of a massive body is indeed very useful for many practical purposes which include spacecraft navigation, geodesic study and time transfer. However, weak deflection itself cannot provide sufficient bounds on these parameters and the geodesic motion of stars around this BH, which is also confirmed by various studies. The authors [51] studied the direct detection of the in-plane Schwarzschild precession around Sgr A^* in the Galactic Center which is fully consistent with GR. Moreover, when the minimal resolution length of the Generalized Uncertainty Principle (GUP) black hole approaches the critical value, it becomes easily unbound due to any disturbance [52]. The authors [53] studied the periastron precession for massive objects orbiting the Lee–Wick black holes and obtained the initial bound on the UV scale of the orbit of the S2 star around Sgr A^* . The preliminary bounds on the charge and bounce parameter were also studied by [54], where the authors used the precession of the S2 star around Sgr A^* detected by gravity.

The gravitational deflection of light in the Sagittarius A^* system has been the subject of ongoing research to test the predictions of both Einstein gravity and Hořava–Lifshitz gravity. In Hořava–Lifshitz gravity, the deflection of light can differ from that predicted by Einstein gravity due to the anisotropic scaling between space and time. The precise deflection of light in the Sgr A^* system would depend on the mass and distribution of the massive objects in the system, as well as the distance and trajectory of the light source. This massive object of our study can be a black hole, wormhole or any compact object. It is also observed that the deflection angle in HL gravity could be larger or smaller than that predicted by Einstein gravity, depending on the parameters of the theory. Further, the deflection angle in this theory could be significantly different from that predicted by Einstein gravity, with the magnitude of the deviation depending on the mass and distance of the massive object. However, it is worth noting that the effects of HL gravity on the gravitational deflection of light in the Sgr A^* system may be small and difficult to observe with the current technology. More detailed calculations and models of the system would

be needed to make precise estimations of the deflection in the context of HL gravity. One may further extend our study to investigate the behavior of the HR parameters in the propagation of electro-magnetic signals between any two regions of spacetime.

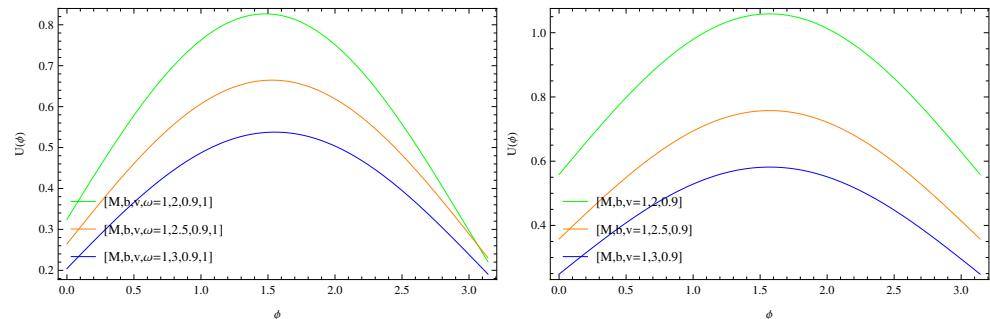


Figure 2. (left) Trajectory of the particle is shown, i.e., $U(\phi)$ against ϕ for different values of the impact parameter b . (right) $U(\phi)$ is shown against ϕ for different values of the impact parameter b , for Schwarzschild case.

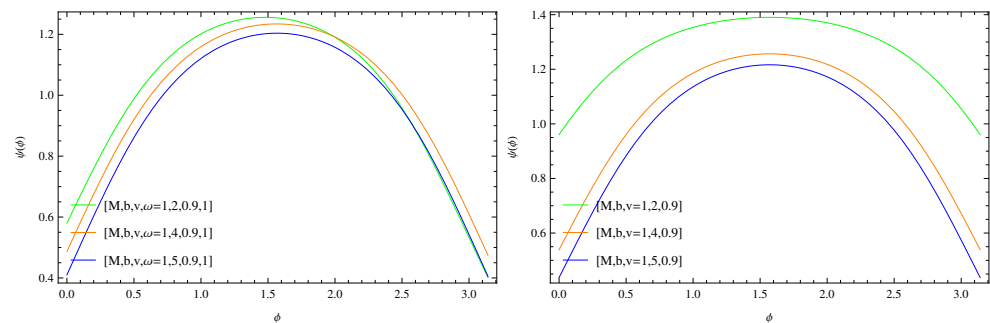


Figure 3. (left) The variation in the angle between radial direction and direction of the particle motion is shown, i.e., $\psi(\phi)$ against ϕ for different values of the impact parameter b . (right) $\psi(\phi)$ is shown against ϕ for different values of the impact parameter b for Schwarzschild case.

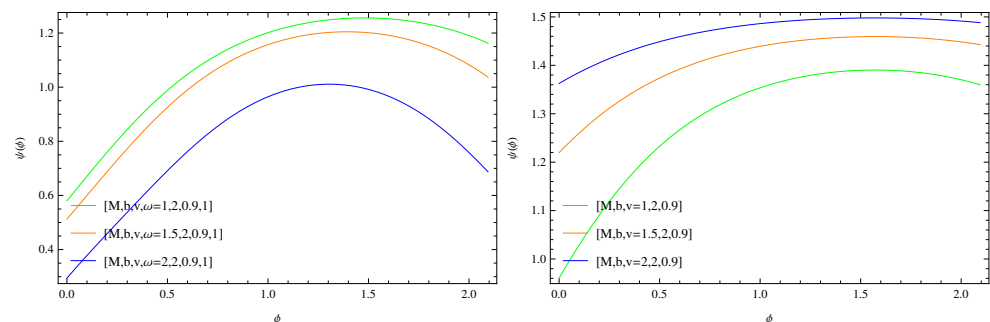


Figure 4. (left) The variation in the angle between radial direction and direction of the particle motion is shown, i.e., $\psi(\phi)$ is shown against ϕ for different values of M of the gravitating body. (right) $\psi(\phi)$ is shown against ϕ for different values of M of the gravitating body, for Schwarzschild case.

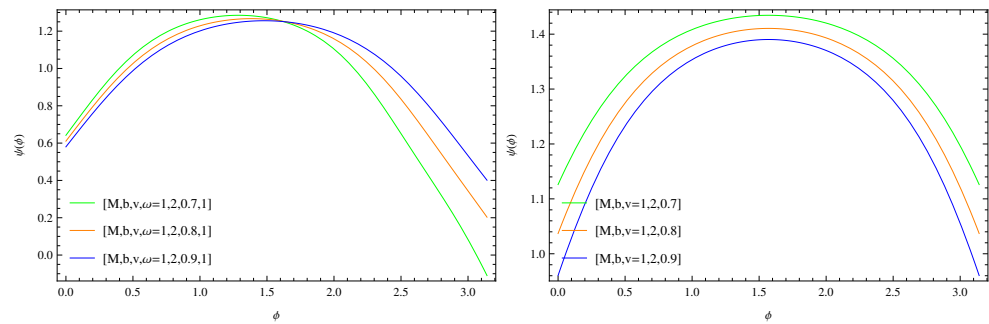


Figure 5. (left) The variation in the angle between radial direction and direction of the particle motion is shown, i.e., $\psi(\phi)$ is shown against ϕ for different values of v . (right) $\psi(\phi)$ is shown against ϕ for different values of v , for Schwarzschild case.

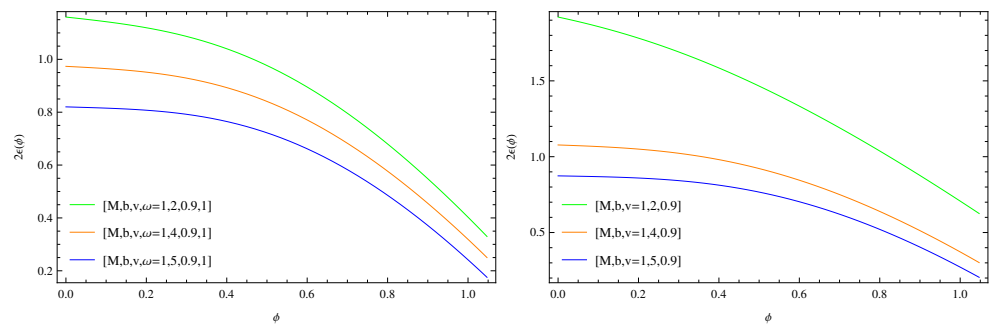


Figure 6. (left) Total deflection $2\epsilon(\phi)$ is shown against ϕ for different values of the impact parameter b . (right) Total deflection $2\epsilon(\phi)$ is shown against ϕ for different values of the impact parameter b , for Schwarzschild case.

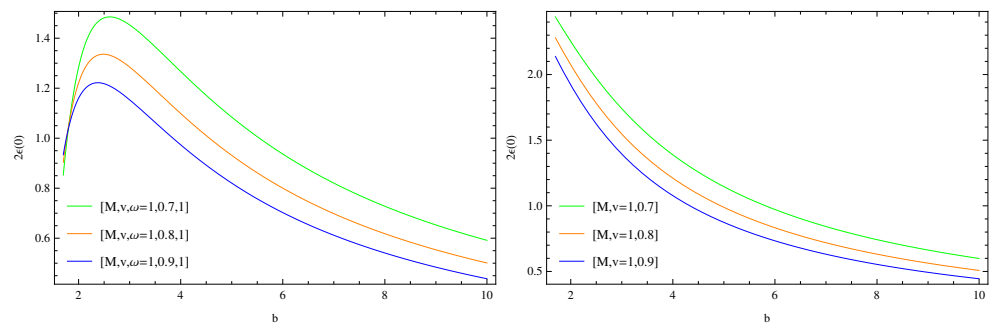


Figure 7. (left) Total deflection for a specific value of ϕ , say, $\phi = 0$, i.e., $2\epsilon(0)$ is shown against the impact parameter b for different values of v . (right) Total deflection $2\epsilon(0)$ at $\phi = 0$ is shown against the impact parameter b for different values of v , for Schwarzschild case.

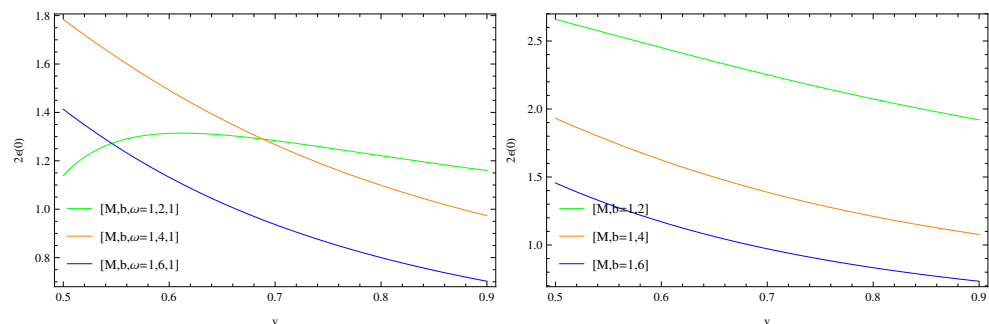


Figure 8. (left) Total deflection for a specific value of ϕ , say, $\phi = 0$, i.e., $2\epsilon(0)$ is shown against v for different values of the impact parameter b . (right) Total deflection $2\epsilon(0)$ at $\phi = 0$ is shown against v for different values of the impact parameter b , for Schwarzschild case.

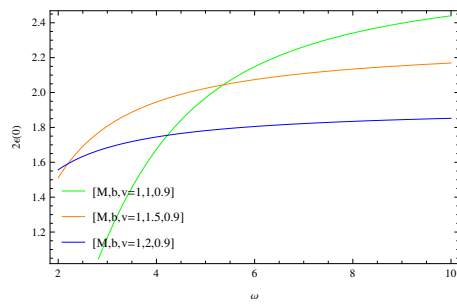


Figure 9. The variation in the total deflection $2\epsilon(0)$ at $\phi = 0$ with respect to the coupling constant ω for different values of the impact parameter b .

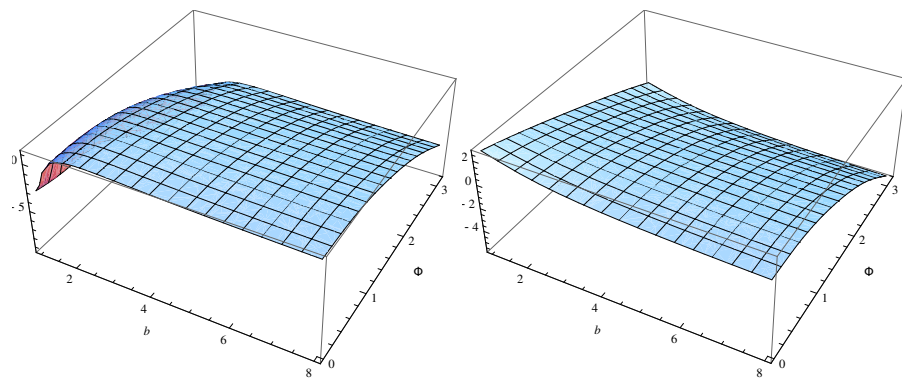


Figure 10. (left) The variation in total deflection 2ϵ is shown with respect to b and ϕ . (right) Total deflection 2ϵ is shown with respect to b and ϕ , for Schwarzschild case.

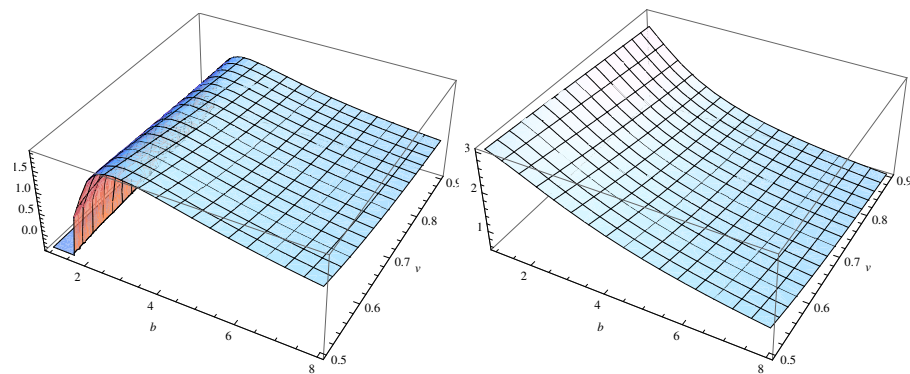


Figure 11. (left) The variation in total deflection $2\epsilon(0)$ at $\phi = 0$ is shown with respect to b and v . (right) Total deflection $2\epsilon(0)$ at $\phi = 0$ is shown with respect to b and v , for Schwarzschild case.

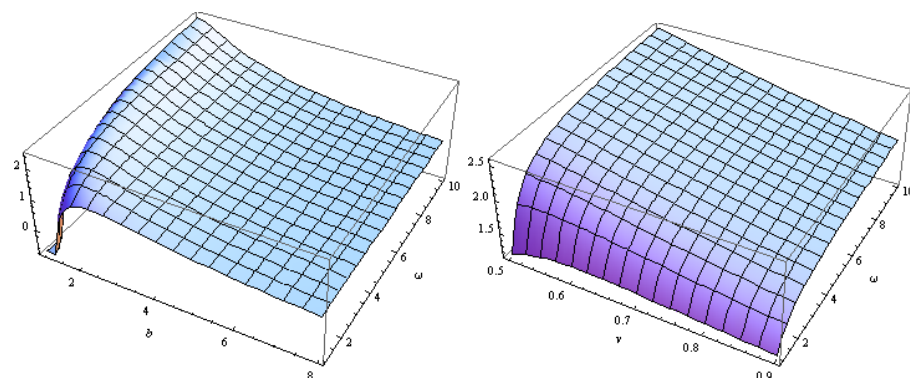


Figure 12. (left) The variation in total deflection $2\epsilon(0)$ at $\phi = 0$ is shown with respect to b and ω . (right) Total deflection $2\epsilon(0)$ at $\phi = 0$ is shown with respect to b and ω .

Author Contributions: Conceptualization, S.I. and F.R.; Methodology, S.I. and F.R.; Software, S.I.; Formal analysis, S.I. and F.R.; Investigation, S.I. and F.R.; Resources, S.I.; Data curation, F.R.; Writing—original draft, F.R.; Writing—review and editing, S.I.; Visualization, F.R. All authors have read and agreed to the published version of the manuscript.

Funding: This work is supported by the Deanship of Scientific Research, Vice Presidency for Graduate Studies and Scientific Research, King Faisal University, Saudi Arabia, under the Ambitious Researcher Track (Project No. GRANT2299).

Data Availability Statement: Not applicable.

Acknowledgments: F.R. would like to thank the Inter-University Centre for Astronomy and Astrophysics (IUCAA), Pune, India, for their hospitality during a visit under the Associateship programme. SI is thankful to his son Md. Aftab Ali for some useful discussions about Sagittarius A* system appearing in the paper. The authors are thankful to all the referees.

Conflicts of Interest: The authors declare no conflict of interest.

References

1. Hořava, P. Membranes at quantum criticality. *J. High Energy Phys.* **2009**, *2009*, 020. [[CrossRef](#)]
2. Jafarzade, K.; Sadeghi, J. Phase transition and holographic in modified Hořava-Lifshitz black hole. *Int. J. Mod. Phys. D* **2017**, *26*, 1750138. [[CrossRef](#)]
3. Hořava, P. Quantum gravity at a Lifshitz point. *Phys. Rev. D* **2009**, *79*, 084008. [[CrossRef](#)]
4. Hořava, P. Spectral Dimension of the Universe in Quantum Gravity at a Lifshitz Point. *Phys. Rev. Lett.* **2009**, *102*, 161301. [[CrossRef](#)]
5. Hořava, P. Quantum criticality and Yang-Mills gauge theory. *Phys. Lett. B* **2010**, *694*, 172. [[CrossRef](#)]
6. Xu, H.; Ong, Y.C. Black hole evaporation in Hořava-Lifshitz gravity. *Eur. Phys. J. C* **2020**, *80*, 679. [[CrossRef](#)]
7. Myung, Y.S. Lifshitz black holes in the Hořava-Lifshitz gravity. *Phys. Lett. B* **2010**, *690*, 534. [[CrossRef](#)]
8. Myung, Y.S.; Kim, Y.W. Thermodynamics of Hořava-Lifshitz black holes. *Eur. Phys. J. C* **2010**, *68*, 265. [[CrossRef](#)]
9. Sadeghi, J.; Banijamali, A.; Reisi, E. Tunneling in Hořava-Lifshitz black hole. *Can. J. Phys.* **2013**, *91*, 64. [[CrossRef](#)]
10. Kiritsis, E.; Kofinas, G. On Hořava-Lifshitz “Black Holes”. *J. High Energy Phys.* **2010**, *122*, 2010. [[CrossRef](#)]
11. Rindler, W.; Ishak, M. Contribution of the cosmological constant to the relativistic bending of light revisited. *Phys. Rev. D* **2007**, *76*, 043006. [[CrossRef](#)]
12. Rahaman, F.; Kuhfittig, P.K.F.; Kalam, M.; Usmani, A.A.; Ray, S. A comparison of Hořava-Lifshitz gravity and Einstein gravity through thin-shell wormhole construction. *Class. Quantum Gravity* **2011**, *28*, 155021. [[CrossRef](#)]
13. Manna, T.; Samanta, B.; Ali, A.; Rahaman, F. Solar system tests in Einstein-ther gravity. *Can. J. Phys.* **2021**, *99*, 8. [[CrossRef](#)]
14. Sultana, P. Contribution of the cosmological constant to the bending of light in Kerr-de Sitter spacetime. *Phys. Rev. D* **2013**, *88*, 042003. [[CrossRef](#)]
15. Soldner, J.G.V. On the Deflection of a Light Ray from its Rectilinear Motion. *Berl. Astron. Jahrb.* **1804**, 161–172, 1804.
16. Jusufi, K.; Sarkar, N.; Rahaman, F.; Banerjee, A.; Hansraj, S. Deflection of light by black holes and massless wormholes in massive gravity. *Eur. Phys. J. C* **2018**, *78*, 349. [[CrossRef](#)]
17. Sultana, J.; Kazanas, D. Bending of light in conformal Weyl gravity. *Phys. Rev. D* **2010**, *81*, 127502. [[CrossRef](#)]
18. Eiroa, E.F.; Romero, G.E.; Torres, D.F. Reissner-Nordström black hole lensing. *Phys. Rev. D* **2002**, *66*, 024010. [[CrossRef](#)]
19. Tsukamoto, N. Deflection angle in the strong deflection limit in a general asymptotically flat, static, spherically symmetric spacetime. *Phys. Rev. D* **2017**, *95*, 064035. [[CrossRef](#)]
20. Lu, X.; Yang, F.W.; Xie, Y. Strong gravitational field time delay for photons coupled to Weyl tensor in a Schwarzschild black hole. *Eur. Phys. J. C* **2016**, *76*, 357. [[CrossRef](#)]
21. Zhao, S.S.; Xie, Y. Strong deflection gravitational lensing by a modified Hayward black hole. *Eur. Phys. J. C* **2017**, *77*, 272. [[CrossRef](#)]
22. Horváth, Z.; Gergely, L.Á.; Keresztes, Z.; Harko, T.; Lobo, F.S. Constraining Hořava-Lifshitz gravity by weak and strong gravitational lensing. *Phys. Rev. D* **2011**, *84*, 083006. [[CrossRef](#)]
23. Eiroa, E.F.; Sendra, C.M. Gravitational lensing by massless braneworld black holes. *Phys. Rev. D* **2012**, *86*, 083009. [[CrossRef](#)]
24. Zhao, S.S.; Xie, Y. Strong deflection lensing by a Lee-Wick black hole. *Phys. Lett. B* **2017**, *774*, 357–361. [[CrossRef](#)]
25. Zhu, X.Y.; Xie, Y. Strong deflection gravitational lensing by a Lee-Wick ultracompact object. *Eur. Phys. J. C* **2020**, *80*, 444. [[CrossRef](#)]
26. Gao, Y.X.; Xie, Y. Strong deflection gravitational lensing by an Einstein-Lovelock ultracompact object. *Eur. Phys. J. C* **2022**, *82*, 162. [[CrossRef](#)]
27. Zhao, S.S.; Xie, Y. Strong field gravitational lensing by a charged Galileon black hole. *J. Cosmol. Astropart. Phys.* **2016**, *2016*, 07. [[CrossRef](#)]
28. Keeton, C.R.; Petters, A.O. Formalism for testing theories of gravity using lensing by compact objects: Static, spherically symmetric case. *Phys. Rev. D* **2005**, *72*, 104006. [[CrossRef](#)]

29. Keeton, C.R.; Petters, A.O. Formalism for testing theories of gravity using lensing by compact objects. II. Probing post-post-Newtonian metrics. *Phys. Rev. D* **2006**, *73*, 044024. [[CrossRef](#)]
30. Keeton, C.R.; Petters, A.O. Formalism for testing theories of gravity using lensing by compact objects. III. Braneworld gravity. *Phys. Rev. D* **2006**, *73*, 104032. [[CrossRef](#)]
31. Liu, F.Y.; Mai, Y.F.; Wu, W.Y.; Xie, Y. Probing a regular non-minimal Einstein-Yang-Mills black hole with gravitational lensings. *Phys. Lett. B* **2019**, *795*, 475–481. [[CrossRef](#)]
32. Lu, X.; Xie, Y. Weak and strong deflection gravitational lensing by a renormalization group improved Schwarzschild black hole. *Eur. Phys. J. C* **2019**, *79*, 1016. [[CrossRef](#)]
33. Lu, X.; Xie, Y. Time delay of photons coupled to Weyl tensor in a regular phantom black hole. *Eur. Phys. J. C* **2020**, *80*, 625. [[CrossRef](#)]
34. Gao, Y.X.; Xie, Y. Gravitational lensing by hairy black holes in Einstein-scalar-Gauss-Bonnet theories. *Phys. Rev. D* **2021**, *103*, 043008. [[CrossRef](#)]
35. Lu, X.; Xie, Y. Gravitational lensing by a quantum deformed Schwarzschild black hole. *Eur. Phys. J. C* **2021**, *81*, 627. [[CrossRef](#)]
36. Wang, C.Y.; Shen, Y.F.; Xie, Y. Weak and strong deflection gravitational lensings by a charged Horndeski black hole. *JCAP* **2019**, *04*, 22. [[CrossRef](#)]
37. Deng, X.M. Probing $f(T)$ gravity with gravitational time advancement. *Class. Quantum Gravity* **2018**, *35*, 175013. [[CrossRef](#)]
38. Zhang, J.; Xie, Y. Gravitational lensing by a black-bounce-Reissner-Nordström spacetime. *Eur. Phys. J. C* **2022**, *82*, 471. [[CrossRef](#)]
39. Cao, W.G.; Xie, Y. Weak deflection gravitational lensing for photons coupled to Weyl tensor in a Schwarzschild black hole. *Eur. Phys. J. C* **2018**, *78*, 191. [[CrossRef](#)]
40. Cheng, X.T.; Xie, Y. Probing a black-bounce, traversable wormhole with weak deflection gravitational lensing. *Phys. Rev. D* **2021**, *103*, 064040. [[CrossRef](#)]
41. Harko, T.; Kovács, Z.; Lobo, F.S.N. Solar System tests of Hořava-Lifshitz gravity. *Proc. R. Soc. A* **2011**, *467*, 1390–1407. [[CrossRef](#)]
42. Turyshev, V.G. Relativistic gravitational deflection of light and its impact on the modeling accuracy for the Space Interferometry Mission. *Astron. Lett.* **2009**, *35*, 215–234. [[CrossRef](#)]
43. Ong, Y.C.; Chen, P. Stability of Hořava-Lifshitz Black Holes in the Context of AdS/CFT. *Phys. Rev. D* **2011**, *84*, 104044. [[CrossRef](#)]
44. Cai, R.G.; Cao, L.M.; Ohta, N. Thermodynamics of black holes in Hořava-Lifshitz gravity. *Phys. Lett. B* **2009**, *679*, 504–509. [[CrossRef](#)]
45. Atamurotov, F.; Abdujabbarov, A.; Ahmedov, B. Shadow of rotating Hořava-Lifshitz black hole. *Astrophys. Space Sci.* **2013**, *348*, 179–188. [[CrossRef](#)]
46. Sadeghi, J.; Jafarzade, K.; Pourhassan, B. Thermodynamical Quantities of Hořava-Lifshitz Black. *Int. J. Theor. Phys.* **2012**, *51*, 3891–3902. Hole [[CrossRef](#)]
47. Kehagias, A.; Sfetsos, K. The black hole and FRW geometries of non-relativistic gravity. *Phys. Lett. B* **2009**, *678*, 123. [[CrossRef](#)]
48. Lu, H.; Mei, J.; Pope, C.N. Solutions to Hořava Gravity. *Phys. Rev. Lett.* **2009**, *103*, 091301. [[CrossRef](#)]
49. Gibbons, G.W.; Werner, M.C. Applications of the Gauss Bonnet theorem to gravitational lensing. *Class. Quantum Gravity* **2009**, *25*, 235009. [[CrossRef](#)]
50. He, G.; Zhou, X.; Feng, Z.; Mu, X.; Wang, H.; Li, W.; Pan, C.; Lin, W. Gravitational deflection of massive particles in Schwarzschild-deSitter spacetime. *Eur. Phys. J. C* **2020**, *80*, 835. [[CrossRef](#)]
51. Abuter, R.; Amorim, A.; Bauböck, M.; Berger, J.P.; Bonnet, H.; Brandner, W.; Cardoso, V.; Clénet, Y.; De Zeeuw, P.T.; Dexter, J.; et al. Detection of the Schwarzschild precession in the orbit of the star S2 near the Galactic centre massive black hole. *Astron. Astrophys.* **2020**, *636*, L5. [[CrossRef](#)]
52. Zhang, J.; Xie, Y. Probing a self-complete and Generalized-Uncertainty-Principle black hole with precessing and periodic motion. *Astrophys. Space Sci.* **2022**, *367*, 17. [[CrossRef](#)]
53. Lin, H.Y.; Deng, X.M. Precessing and periodic orbits around Lee–Wick black holes. *Eur. Phys. J. Plus* **2022**, *137*, 176.
54. Zhang, J.; Xie, Y. Probing a black-bounce-Reissner-Nordström spacetime with precessing and periodic motion. *Eur. Phys. J. C* **2022**, *82*, 854. [[CrossRef](#)]

Disclaimer/Publisher’s Note: The statements, opinions and data contained in all publications are solely those of the individual author(s) and contributor(s) and not of MDPI and/or the editor(s). MDPI and/or the editor(s) disclaim responsibility for any injury to people or property resulting from any ideas, methods, instructions or products referred to in the content.